

The field-dependent viscoelastic and transient responses of plate-like carbonyl iron particle based magnetorheological greases

Journal of Intelligent Material Systems and Structures

2019, Vol. 30(5) 788–797

© The Author(s) 2019

Article reuse guidelines:

sagepub.com/journals-permissions

DOI: 10.1177/1045389X19828504

journals.sagepub.com/home/jim



Norzilawati Mohamad¹ , Saiful Amri Mazlan¹, Ubaidillah², Seung-Bok Choi³ , Fitriani Imaduddin⁴ and Siti Aishah Abdul Aziz¹

Abstract

The field-dependent viscoelastic and transient behaviours of plate-like-carbonyl-iron-particle-based magnetorheological greases are experimentally investigated in this study. The plate-like carbonyl-iron particles are made from spherical carbonyl-iron particles through a milling process using a rotary ball mill. Several samples of magnetorheological greases consisting of different weight percentages of plate-like carbonyl-iron particles are prepared. The surface microstructures and distributions of the plate-like carbonyl-iron particles in the grease are observed using various types of microscopic investigations. Subsequently, the viscoelastic and transient (dynamic) rheological properties of the plate-like carbonyl-iron particles are investigated using a commercial rheometer. The spherical carbonyl-iron particles are transformed into the flattened plate-like carbonyl-iron particles with a larger surface diameter. It is shown that the viscoelastic properties such as storage modulus and response time of the plate-like carbonyl-iron particles significantly depend on the shape and particle weight fraction. The findings reveal that the shape of the carbonyl-iron particles has a significant effect on the field-dependent behaviours. Thus, the results presented in this work provide very useful scientific contributions for devising appropriate applications utilizing the plate-like-carbonyl-iron-particle-based magnetorheological greases.

Keywords

Magnetorheological grease, transient response, spherical particle, plate-like particle, microstructure, viscoelastic properties

1. Introduction

For last two decades, several different types of magnetorheological (MR) materials have been developed and are classified as an intelligent materials; their properties can be changed reversibly and continuously by an external magnetic field within milliseconds (de Vicente et al., 2011). Owing to these desirable properties, the studies related to MR materials attract a significant attention. In recent years, these materials have been employed in various industrial areas including the automotive industry (Carlson and Jolly, 2000; Ichwan et al., 2016; Imaduddin et al., 2014; Park et al., 2010; Ubaidillah et al., 2014). Each MR material has its own advantages and also disadvantages over different MR materials. The most common MR material is MR fluid invented by Rabinow (1948). MR fluid has salient features such as fast response time and high MR effect. However, despite the successful application to real vehicles as semi-active dampers, currently available MR fluid faces

severe sedimentation and leakage problem, which directly limit its effective usage in many other practical

¹AVS Research Laboratory, Malaysia-Japan International Institute of Technology, Universiti Teknologi Malaysia, Kuala Lumpur, Malaysia

²Mechanical Engineering Department, Faculty of Engineering, Universitas Sebelas Maret, Surakarta, Indonesia

³Smart Structures and Systems Laboratory, Department of Mechanical Engineering, Inha University, Incheon, Korea

⁴Faculty of Engineering and Technology, Multimedia University, Bukit Beruang, Malaysia

Corresponding authors:

Saiful Amri Mazlan, AVS Research Laboratory, Malaysia-Japan International Institute of Technology, Universiti Teknologi Malaysia, Jalan Sultan Yahya Petra, 54000 Kuala Lumpur, Malaysia.
Email: amri.kl@utm.my

Seung-Bok Choi, Smart Structures and Systems Laboratory, Department of Mechanical Engineering, Inha University, 253 Yonghyun, Namgu, Incheon 402-751, Korea.
Email: seungbok@inha.ac.kr

applications (Gómez-Ramírez et al., 2009; López-López et al., 2008). In order to overcome the problems of MR fluid, MR elastomer was introduced and extensively studied in terms of material characterization and applications such as vibration isolator. However, MR elastomer exhibits relatively low MR effect compared with MR fluid because of the difficulty of achieving uniform distributions of the high-intensity magnetic field (Rigbi and Jilkén, 1983). Therefore, a new class of MR materials called MR grease was recently introduced to overcome the problems of MR fluid and MR elastomer. MR grease was discovered by Rankin et al. (1999). They introduced a controllable grease as a viscoplastic medium in MR fluid domain to reduce the sedimentation problem as well as improve the MR effect. Now, MR grease is known as an intermediate material between MR fluid and MR elastomer, which has a high viscoelastic property as a medium for the dispersion of carbonyl-iron (CI) particles. Several works on MR grease have demonstrated that there is no sedimentation problem due to the high off-state viscosity attributed by the grease medium and MR effect is relatively high compared with MR elastomer (Kintz et al., 2003; Mohamad et al., 2016; Park et al., 2011; Sahin et al., 2007). This salient property of MR grease is advantageous over MR fluid in terms of the sedimentation and over MR elastomer in terms of MR effect. However, it has been also identified that the response time of MR grease is slow compared with MR fluid (Gordaninejad et al., 2007; Kavlicoglu et al., 2013; Sarkar et al., 2015; Sukhwani and Hirani, 2008). These previous works on MR greases indicate that appropriate application devices or systems should be different from those using MR fluid or MR elastomer.

Recently, the research on MR grease is actively being undertaken, but most studies on MR greases have focused only on the preparation of certain samples and experimental investigations of their field-dependent rheological properties. Park et al. (2011) studied the rheological behaviour of an MR grease under various magnetic fields and showed that a high yield stress could be achieved due to the intrinsic grease property. The study was continued by investigating the temperature effect on the yield stress of MR grease by Sahin et al. (2009). The yield stress was decreased by approximately 77% by increasing the temperature up to 70°C at a current of 2 A. In addition, the influence of different weight percentages of CI particles utilized in MR grease was investigated by Mohamad et al. (2016), showing that 70 wt% of CI particles can provide the highest yield stress and MR effect. The influence of an additive in MR grease was also investigated to reduce the off-state viscosity and improve on-state yield stress (Kim et al., 2012; Song et al., 2009). The results have shown that the off-state viscosity and the yield stress are reduced by adding kerosene oil to MR grease. It has also been shown that the addition of

nanoparticle additives to MR grease can improve the stability of the viscoelastic medium without a significant reduction of the yield stress. It is noted here that all of these previous studies on MR greases have investigated the field-dependent rheological properties of MR greases containing spherical CI particles.

Studies of different shapes of CI particles in an MR fluid have been extensively performed. Advantages of using the plate-like shape of CI particles over the spherical shape of CI particles have been identified as the larger induced magnetic moment owing to their smaller demagnetization factor in their long direction, and anisotropy axes which directly enhance the field-dependent yield stress of MR fluids (de Vicente et al., 2010). The plate-like CI particles are easily magnetized at a low magnetic field since the long axis is aligned along the external magnetic field applied to form stable chain structures (Shah et al., 2014). As a consequence, improvements in the rheological properties and yield stress have been achieved (de Vicente et al., 2009). In addition, the stability of the suspension is significantly dependent on the shape of the CI particles, which is a crucial issue in MR applications (de Vicente et al., 2010). For example, Upadhyay et al. (2014) studied the rheological properties focusing on the storage modulus of the plate-like-CI-particle-based MR fluid and compared them with those of the spherical CI-particle-based MR fluid. The results have shown that the plate-like-CI-particle-based MR fluid provides a higher storage modulus (6 MPa) at a low magnetic field, compared to the spherical-particle-based MR fluid. It has been investigated that the plate-like CI particles can produce a higher yield stress with a larger diameter of the particles (Shah et al., 2013). In addition, the plate-like-CI-particle-based MR fluid can reduce the sedimentation rate by 20% compared with the spherical CI particles (Shilan et al., 2016). The above-mentioned advantages of the plate-like-CI-particle-based MR fluid can enhance the feasibility of practical applications such as damper, valve, mount and clutch (Ubaidillah et al., 2014; Ichwan et al., 2016). In applications of MR fluids or MR greases, the transient response is also one of the crucial factors to be considered since it is directly related to the field-dependent dynamic properties of the application devices or systems. This can contribute to the development of the most adaptable application with proper MR fluids or MR greases. In addition, the transient behaviour is very important to understand the structuring process of the suspended CI particles in the grease medium.

However, despite several works on the transient responses of MR fluids, there is no report on the transient responses of an MR grease, especially with the plate-like CI particles. Consequently, the technical novelty and scientific contribution are to experimentally investigate the transient response of MR greases and identify the behaviour from the physical aspect of

MR greases. In order to achieve this research goal, five different samples with different weights of CI particles are prepared using a ball mill machine. Particle characterizations including analyses of the particle size and pattern are performed using the field-emission scanning electron microscopy. Subsequently, the surface and shapes of the particles are visually observed using a three-dimensional (3D)-laser microscope followed by an investigation of the field-dependent rheological properties such as storage modulus. Then, the transient rheological dynamics of the plate-like CI particles are evaluated to understand the response time to the external magnetic field, which is one of the crucial factors in practical applications of MR grease. Specially, the transient response is closely related to control devices or circuits to achieve desired performances of the application systems, which is called control bandwidth of the application device of MR greases.

2. Measurement methodology

2.1. Sample preparation

Experiments were performed using two different shapes of CI particles suspended in a commercial grease medium. Six samples of MR grease with various concentrations of plate-like and spherical CI particles were prepared. The grease used in this study was based on lithium, with a viscosity of 147.8 mPa s at 40°C. The spherical CI particles with an average diameter in the range of 3.9–5.2 μm and density of 7.874 g cm^{-3} were purchased from BASF, Germany. The plate-like CI particles were fabricated from commercial spherical CI particles through a mechanical alloying process using a high-energy rotary ball mill machine at a rotational speed of 180 r/min for 40 h using zirconia ball at a ball-to-powder weight ratio of 20:1. Therefore, the obtained plate-like CI particles were dispersed in the grease medium using a mechanical stirrer to produce the MR grease. The samples were stirred for 2 h at a speed of 300 r/min to obtain a homogeneous plate-like-CI-particle-based MR grease (MRGP). The samples were prepared with plate-like-CI-particle concentrations of 70, 60, 50, 40 and 30 wt%. The spherical-CI-particle-based MR grease (MRGS) was prepared only with a concentration of 70 wt% as a reference sample for a comparative analysis.

2.2. Characterization

The surface morphologies and average diameters of the plate-like and CI particles were investigated using a field-emission scanning electron microscope (FESEM, JSM-7800F, JEOL) and laser diffraction particle size analyser (SALD-2300, Shimadzu). A 3D-laser microscope (LEXT OLS4100, OLYMPUS) was used to determine the thickness of the particles in order to

calculate the aspect ratio ($a_r = d/L$). A Fourier-transform infrared (FTIR; Cary 600 Series, Agilent Technologies) was used to confirm the chemical structures of the unmilled (spherical) and milled (plate-like) CI particles. The spectra were collected in a wavelength range of 500–4000 cm^{-1} at room temperature. In addition, an environmental scanning electron microscope (ESEM; Quanta 450 FEG, FEI) was used to clearly observe the homogeneous distributions of the spherical and plate-like CI particles in the grease medium.

The viscoelastic properties of the MRGP samples were characterized at the oscillatory mode using parallel-plate configuration of a rotational magnetorheometer (MCR 302, Anton Paar). A parallel-plate diameter of 20 mm and constant gap distance of 1 mm using a magnetorheological device (MRD) 70 were employed for the on-state measurement. The on-state measurement was performed at a magnetic setting of 0–5 A corresponding to the range of 0–700 mT. The energy storage, G' and loss modulus, G'' were measured at an excitation frequency of 1 Hz and strain amplitude of 0.1%. In addition, the transient responses under a stepwise magnetic field of the MRGS and MRGP samples were investigated at the maximum applied magnetic field of 0.7 T to understand the response time. The experiment was performed without a magnetic field at the first 120 s; then, a magnetic field of 0.7 T was instantaneously applied to the MRGS and MRGP samples in the following interval of 120 s (time range: 120–240 s) and instantaneously removed at 240 s. The dimensionless storage moduli of the MRGS and MRGP samples were then calculated and analysed.

3. Particle characterization

The sizes of the spherical and plate-like CI particles are confirmed using the FESEM micrographs. Figure 1(a) shows the morphology of the initial state of the particles with a spherical shape. Figure 1(b) shows the flattened shape of the CI particles after the ball milling process. The flattened shape emerged owing to the collisions between the CI particles powder and the zirconia ball in the presence of ethanol, which led to a breaking of the cluster form of the CI particles (Shilan et al., 2016). Furthermore, the results reveal a more homogeneous distribution of the plate-like CI particles and wetted surface area, compared to the spherical CI particles. The mean diameter and standard deviation of the plate-like CI particles obtained after the milling process are 6.17 μm and 0.26, respectively, measured using the laser diffraction particle size analyser. The spherical CI particles had a mean diameter of 4.95 μm with standard deviation of 0.2, as shown in Figure 2. The size distributions parameters (Figure 2) had values of $d_{10} = 2.72$, $d_{50} = 4.95$ and $d_{90} = 9.03$ for the

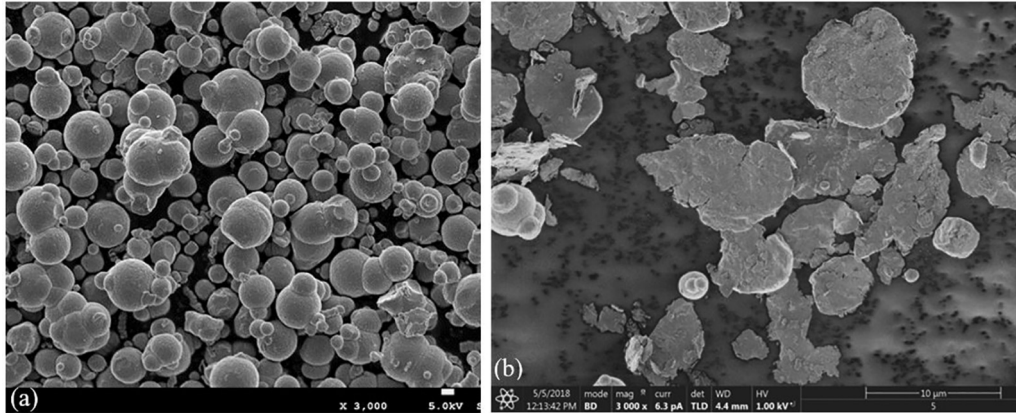


Figure 1. FESEM micrographs of (a) spherical and (b) plate-like CI particles.

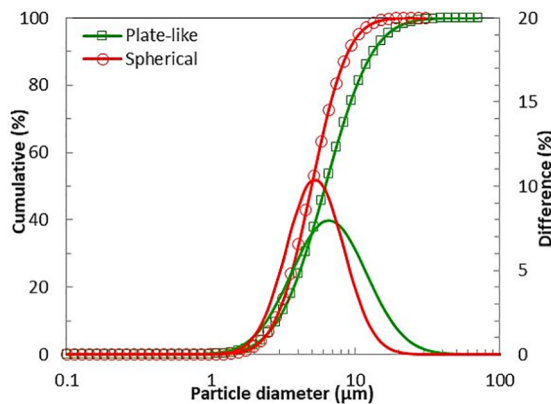


Figure 2. Size analyses of the CI particles with different shapes.

spherical and $d_{10} = 2.84$, $d_{50} = 6.17$ and $d_{90} = 13.38$ for the plate-like CI particles.

Furthermore, the average aspect ratio ($a_r = d/L$) of the plate-like CI particles was calculated; it reached the value of 20, with an average thickness of $0.31 \mu\text{m}$. It is worth noting that according to Wenyan et al. (2015), all of the spherical CI particles were transformed into plate-like CI particles after 40 h of milling at room temperature. This finding has been also supported by the study of Wang et al. (2015), which revealed that the morphology evolution is relatively slow at room temperature, compared to the wet ball milling process. In addition, the morphology evolution of the CI particles in the milling process depends on the processing time and speed rate. The average surface area of the plate-like CI particles becomes larger while the thickness decreases with the milling process proportionally to the time and speed.

Figure 3 shows the transmittance data for the different shapes of CI particles in the range of $500\text{--}3500 \text{ cm}^{-1}$. The unmilled (spherical) and milled (plate-like) CI particles exhibited similar peak characteristics.

Furthermore, the results demonstrated that there are no impurities in the plate-like CI particles, underwent the milling process. The spectrum of the CI particles detected Fe, C and O, embedded in potassium bromide (KBr). The transmittance of the CI particles exhibited features at 3435 , 2090 , 1635 and 719 cm^{-1} . All of the peaks obtained in the wavelength range corresponded to either stretching or bending vibrations belong to the hydrocarbon CI particles components. A difference between the shapes is that the plate-like CI particles exhibited a lower transmitted light intensity in the wavelength range, owing to the oscillating dipole in the plate-like CI particles corresponding to long-wavelength crystal modes; longitudinal and transverse modes were considered (Farmer, 1998). In this case, the infrared (IR) vibration is perpendicular to the plate-like structure, which occurred at their longitudinal frequencies; the dipole is induced from surface charges of the plate-like CI particles. Moreover, a broadened transmission peak and shift to higher frequencies were observed, dependent on the CI particles' size and shape. With the increase in the size of the CI particles, the particles begin to separate and optically appear as a single crystal. Consequently, the sharp edges of the plate-like CI particles easily break during the milling process, leading to less irregular particles, as shown in Figure 1(b) (Luxon et al., 1969).

The CI particles' shapes are further analysed using the 3D-laser microscope to evaluate the surface roughness, as presented in Figure 4(a) and (b). The details of surface roughness comparison between plate-like and spherical CI particles are summarized in Table 1. The analysis revealed that the surface roughness values of the plate-like and spherical CI particles were 1.43 and $1.07 \mu\text{m}$, respectively. This result demonstrates that the plate-like CI particles shape with the larger surface area have higher surface roughness and wetted surface area, which can provide strong mechanical and magnetic

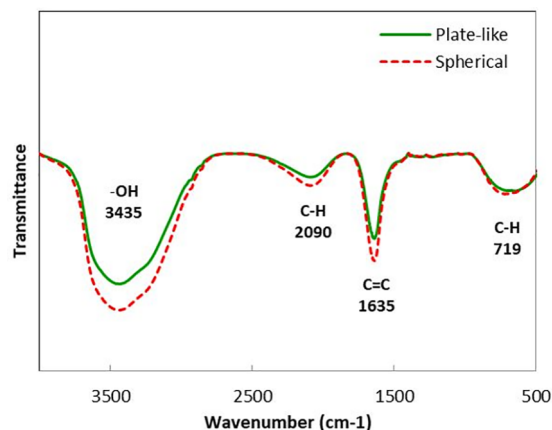


Figure 3. Transmittance patterns of the different shapes of CI particles using FTIR spectroscopy.

interparticle interactions, compared to the spherical CI particle. This phenomenon indirectly enhances the solid surface friction between plate-like particles, which impedes the orientation motion of the particles towards the magnetic field direction (Laherisheth and Upadhyay, 2017; Siebert et al., 2015). The presence of anisotropy axes in the plate-like CI particles improves the interparticle interaction when a magnetic field is applied (Jones and Friedman, 2000; Wang et al., 2015). Therefore, the plate-like CI particles significantly more easily align following the magnetic direction, compared to the spherical CI particles, which tend to align in one direction. In the presence of magnetic field, the plate-like CI particles can produce one or more axes and tend to align in long configuration parallel to the field direction. The strong and stable formation of chain structures attained in the MRGP owing to the anisotropy properties belongs to the plate-like CI particles. Theoretically, the shape anisotropy is easy to be magnetized, however, complex to be demagnetized due to the spatial inhomogeneity of the magnetization (Chekanova et al., 2015). Therefore, a greater retentivity was stimulated for the plate-like CI particles attributable to their easy magnetization axis and smaller demagnetization factor in their long direction (Laherisheth and Upadhyay, 2017; Mohamad et al., 2018). Furthermore, it is expected that the plate-like CI particles will produce high MR effect than spherical CI particles due to their larger surface contact area. The formation of anisotropy shape chain structures can reduce the void between plate-like CI particles, yet increase the solid friction (Siebert et al., 2015). It is noted that the plate-like CI particles have larger storage modulus compared to the spherical CI particles (Upadhyay et al., 2014). Moreover, the external factor such as restriction movement from grease medium should be taken into consideration.

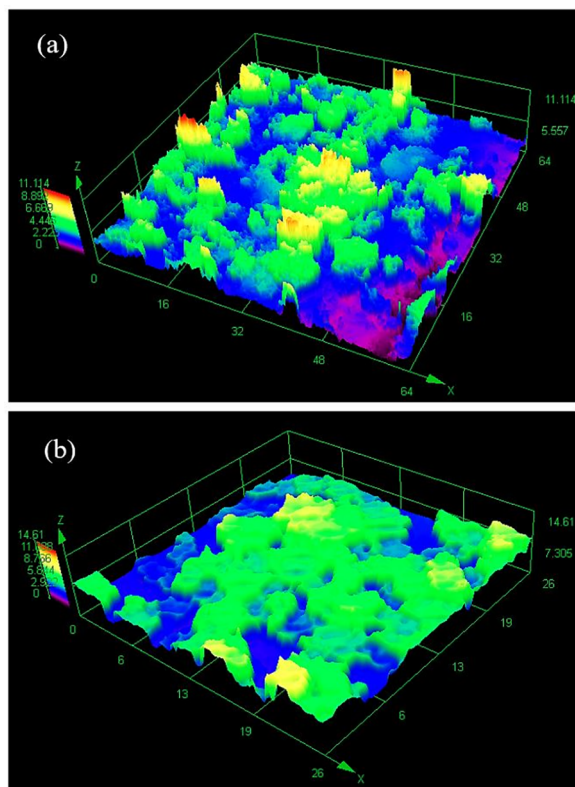


Figure 4. 3D-laser micrographs of (a) plate-like and (b) spherical CI particles.

Figure 5 shows an ESEM micrograph corresponding to the distribution of plate-like and spherical CI particles in the MR grease. In this image, the white spots represent the plate-like CI particles, while the dark background corresponds to the grease medium. This analysis reveals that the plate-like CI particles are uniformly distributed in the grease medium compared to the spherical CI particles shape. The value of surface roughness measured can be used as the reference for the compatibility between different shape of CI particles and grease as medium. The higher surface roughness of the plate-like CI particles will produce stronger adhesion and indirectly improve the bonding between particles and medium (Wilson et al., 2017). This condition leads to the restrictions on the particle's movements in the grease. It has been identified from the experimental results that the kurtosis value, which represents the sharpness of the roughness particles, shows that the plate-like CI particles have spiked ($Sku > 3$) distribution compared to the spherical CI particles ($Sku < 3$). In addition, the adhesion attraction between particles and medium is well represented by the end tip of the particles is in the tilted/skewness particles rather than sphere (Mizes, 1995). The results reveal that the plate-like CI particles has better asperity (degree of the roughness shape) compared to the spherical shape. This

Table 1. Comparison of surface roughness for different shapes of CI particles.

Parameters	Plate-like CI particles	Spherical CI particles
Sa (arithmetical mean height)	1.43 μm	1.07 μm
Sq (root mean square height)	1.659 μm	1.597 μm
Sz (maximum height)	11.027 μm	8.539 μm
Sp (maximum peak height)	7.388 μm	4.636 μm
Sv (maximum pit height)	3.639 μm	3.904 μm
Ssk (skewness)	1.091	0.197
Sku (kurtosis)	4.661	2.646

CI: carbonyl-iron.

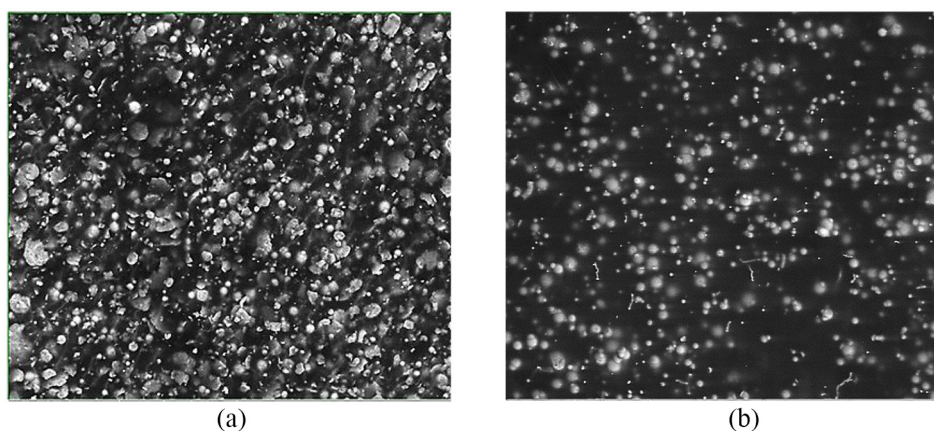


Figure 5. ESEM micrographs corresponding to the distribution of 70 wt%: (a) plate-like and (b) spherical CI particles in the MR grease.

condition implies that a good interfacial compatibility between the plate-like CI particles and grease medium was achieved in the prepared samples.

4. Rheological and transient behaviours

The rheological properties were characterized at room temperature using the magneto-rheometer. The storage modulus values of the different weight percentages of plate-like CI particles at a constant current (2 A) are shown in Figure 6. As expected, the storage modulus increases parallel with the weight percentage of the plate-like CI particles, the larger surface contact area of the plate-like CI particles stimulates stronger the magnetic interparticle interactions. This leads to an enhancement of the friction effect between the interparticle interactions with the increase in the plate-like weight percentage. Therefore, the particles with a larger size tend to align more easily following the magnetic field direction, compared to the particles with a smaller size. In addition, Agirre-Olabide and Elejabarrieta (2017) reported that the storage modulus increases owing to the mechanical reinforcement, emerging from the physical interactions between the plate-like CI particles and grease medium. A higher stiffness of the

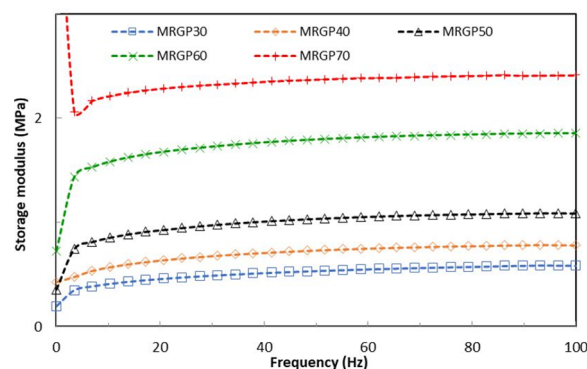


Figure 6. Storage moduli of the MRGP samples for various weight percentages at 2 A.

MRGP can be obtained by increasing the weight percentage of the plate-like CI particles up to the critical particle concentration. This phenomenon reveals that all plate-like CI particles are almost in contact with each other when the external magnetic field is applied.

Figure 7 shows the storage moduli of the MRGP60 samples at input currents in the range of 0–5 A, corresponding to magnetic fields 0–0.7 T. The same pattern was obtained for the other samples. The storage

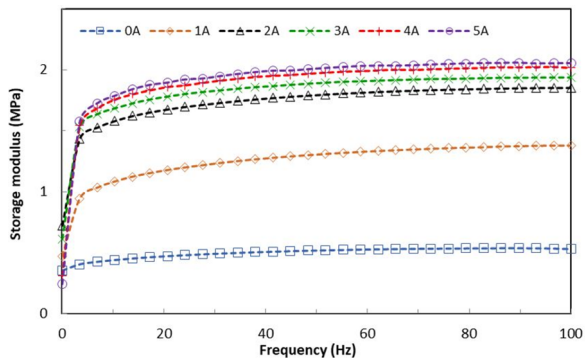


Figure 7. Dependences of the current on the frequency for the MRGP60 sample.

modulus increases with the magnetic field. The chain structure formation in the MRGP has a significant effect on the storage modulus under the external magnetic field. Several studies have shown that plate-like CI particles have a higher remanence and larger coercivity, compared with those of spherical CI particles (Jahan et al., 2017; Laherisheth and Upadhyay, 2017; Siebert et al., 2015; Upadhyay et al., 2014). This enhances the potential of interparticle attractions even in the absence of an external magnetic field. Therefore, the stronger interparticle interactions in the MRGP can be considered as one of the salient merits of the plate-like particles.

The effect of frequency on the storage modulus has been investigated. The graph pattern shows that the storage modulus of the MRGP60 increases rapidly at low frequency ($f < 10$ Hz) and is gradually stabilized with the increase in the frequency. The same pattern is observed for other samples. The increment of the storage modulus as function of frequency represents the enhancement in the elasticity achieved with plate-like CI particles which leads to the stronger and stable chain structures formation. However, by increasing the weight percentages of plate-like CI particles up to 70 wt%, the storage modulus is reduced at low frequency ($f < 10$ Hz). This phenomenon indicates that the interconnected chain structure bonds are ruptured. In addition, the increase in the plate-like-CI particle concentration up to 70 wt% has made the dependency of field behaviour towards the frequency. At the early stage when magnetic field is applied, the high CI particles concentration (MRGP70) exhibits weak-link behaviour, in which the elasticity of the particles cluster is preference. Thus, the increment of the storage modulus in the MRGP70 is lagged with the increase in the frequency (Segovia-Gutiérrez et al., 2012). This condition happened due to the relaxation time of the MRGP70 has moved to the higher value owing to the crossover point between storage modulus and loss modulus which moves to the lower frequency. However, the same trend is less apparent with the magnetic field

applied below than 2 A. This reveals that the interactions of the interparticles during the formation of chain clusters are high with the presence of physical force which represents the bonding. This phenomenon confirms that the MRGP exhibits as the gel or semi-solid behaviour with the presence of external magnetic field (Mohamad et al., 2016).

In order to understand the interaction mechanisms of the particles with different shapes upon the application of the external magnetic field, which are directly related to the response time of the properties' changes upon the input field application, the storage moduli of both shapes in response to the stepwise magnetic field were measured. In this experiment, the MRGP and MRGS samples with the highest weight percentages of CI particles of 70 wt% were utilized. The storage moduli of the MRGP and MRGS samples were measured upon the application of a stepwise magnetic field; a magnetic field of 0.7 T was instantaneously applied to the sample at 120 s and instantaneously removed at 240 s. The transient response experiment was set up by varying the magnetic field as function of time. In addition, the experiment was examined under the linear viscoelastic (LVE) region with constant frequency and strain: 1 Hz and 0.1%, respectively. At first, the sample was exposed to the off-state condition (no magnetic field, 0 Hz and 0 strain) for interval of 120 s. The result showed that the storage modulus remained at 0 in the absence of magnetic field. This proves that the storage modulus is independent of time. Subsequently, the sample was exposed to the on-state condition with the fixed strain, frequency and maximum magnetic field in order to allow the CI particles to construct the stable chain structures in following interval of 120 s. It is observed that the storage modulus increases rapidly and gradually stabilized. As the current was set to 5 A, the coil promptly generated constant magnetic flux density (0.7 T), which can be read by the Gaussmeter. After the step magnetic field was removed (no magnetic field), the storage modulus rapidly decreases and gradually stabilized at 0 for the following interval. The differences between the results of the MRGP and MRGS samples cannot be attributed to the microstructure rupture during implementation of the actuating strain; the strain was set following the LVE region for each sample during the test (Xu et al., 2013; Yang et al., 2017).

Figure 8(a) reveals that the MRGP sample exhibits a rapid and large evolution response of the storage modulus upon the application of the maximum magnetic field at 0.7 T (time range of 120–240 s), compared to the MRGS sample. The formation chain structures of plate-like CI particles can be instantly observed at 120 s upon the application of the magnetic field on the MRGP sample. The anisotropy axes in the plate-like CI particles significantly improved the time response and strengthened the particle chain alignment in the MRGP, leading to a higher storage modulus,

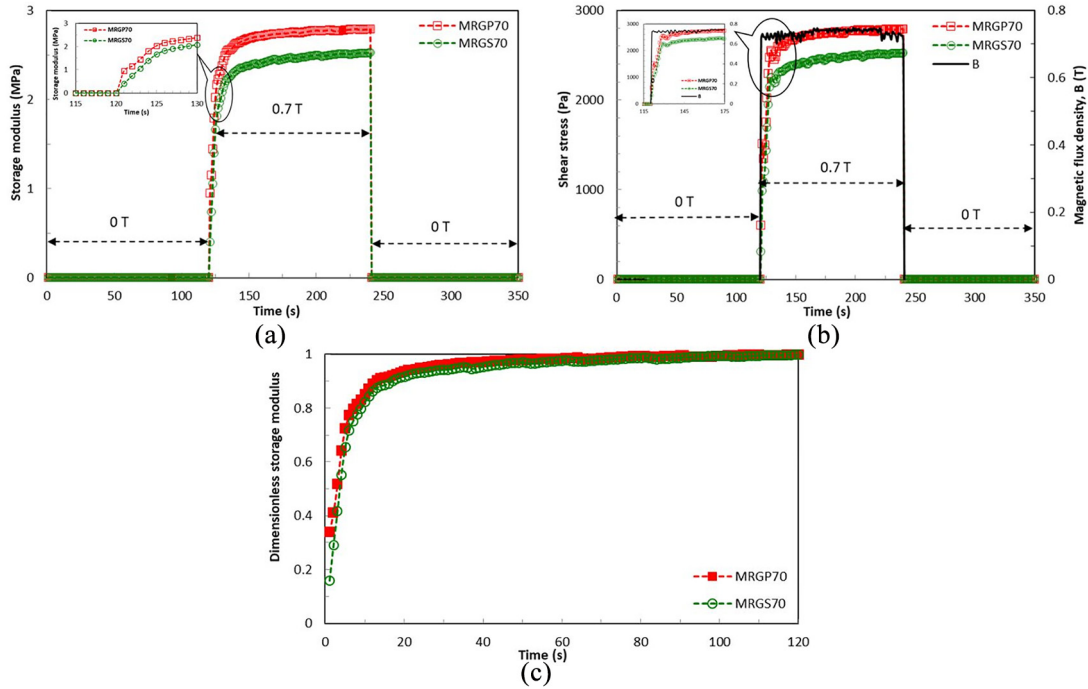


Figure 8. (a) Time dependence of the storage modulus for MR grease upon the application of a stepwise magnetic field. (b) Time dependence of the shear stress and magnetic flux density of MR grease. (c) Dimensionless transient response of the storage modulus under a magnetic field of 0.7 T.

compared with that of the spherical CI particles. Therefore, this demonstrates that the formation of chain structures of the plate-like and spherical CI particles is self-assembling from the random dispersion (Figure 5) along the direction of the magnetic field, which could change the performances of the MRGP and MRGS.

As mentioned above, the plate-like and spherical CI particles dispersed randomly in the grease medium could form stable chain structures along the magnetic field direction by exposure to the external magnetic field for a long time period. Furthermore, the chain structures can be retained for a certain period of time (time range of 120–240 s), as shown in Figure 8(a), before removing the magnetic field and returning to the initial state. This is one of the advantages of the MRGP, in which the CI particles with different shapes could suspend in the grease medium for a long time period against gravitational force (Karis et al., 2003; Mohamad et al., 2016). This has been also confirmed by Carlson (2002), where the stability has been a crucial preference for practical applications without a significant sedimentation problem. The shear stress growth of both MR greases upon application of a stepwise magnetic field is depicted in Figure 8(b). The result shows that MRGP has rapid shear stress growth compared to the MRGS subjected to the same magnetic field and time: 0.7 T and 120 s, respectively. This phenomenon proves that the shape anisotropy of the plate-like CI

particles leads to the formation of stable chain structures with the prompt shear stress growth. This is due to the edge of the plate-like CI particles is more sensitive to be attracted to align following the applied magnetic field direction rather than spherical shape. Figure 8(c) shows the dimensionless transient responses of the storage moduli of the MRGP and MRGS samples under a magnetic field of 0.7 T. The dimensionless storage modulus is calculated as

$$\text{Dimensionless } G' = \frac{G'}{G'_{max}} \quad (1)$$

where G'_{max} is the maximum value of G' for MRGP and MRGS samples in the time range of 120–240 s. This dimensionless transient response of the storage modulus is analysed for a better understanding of the movement of the CI particles in the grease medium by a sudden application of an external magnetic field. Figure 8(c) reveals that the dimensionless storage moduli of the MRGP and MRGS samples increased up to 0.99, defined by the time required for CI particles to align and form stable chain structures. According to Xu et al. (2013), the dimensionless storage modulus fluctuates between 0.99 and 1, which reflects the series of ruptures and reformation process of the chain structures of the MRGP and MRGS samples under the strain oscillatory mode at the maximum magnetic field.

Based on these results, it can be summarized that the orientation and alignment of the chain structures of the

plate-like and spherical CI particles were restricted with the high viscoelastic forces from the grease network. This phenomenon also occurs in MR gels, where the embedded CI particles are restrained in compact chain structures owing to the polymer network forces (An et al., 2012). In addition, MRGP requires a short time period to form stable chain structures, compared to MRGS, owing to the anisotropy axes belonging to the plate-like particles. It is worth noting that the spherical CI particles have a single axis. It can be deduced that by displacement that the plate-like CI particles with anisotropy axes can be easily magnetized and aligned following the high magnetic-field direction; in addition, a short time period is required to form stable chain structures.

5. Conclusion

The surface microstructures and field-dependent rheological properties of plate-like CI particles dispersed in a grease medium were investigated to evaluate transient rheological dynamics. The plate-like CI particles were fabricated using commercial spherical CI particles through a ball milling process. Several samples with various weight percentages (30–70 wt%) of MRGP were prepared to evaluate their rheological properties related to the magnetic field strength using an oscillatory shear rheometer. Significant changes in the shape, diameter and thickness of the plate-like CI particles were observed. Flattened CI particles with an average diameter of 6.17 μm were obtained from the milling process. A better dispersion of the plate-like CI particles in the grease medium was obtained, compared with that of the spherical CI particles. The enhancement of the storage modulus of the MRGP showed that stronger interparticle interactions were formed by the increase in the weight percentage of the plate-like CI particles. In addition, the MRGP exhibited a short response time, compared to the MRGS, owing to the anisotropic axes in the plate-like CI particles. Studies on optimization processes for the particle thickness and size to achieve the maximum storage modulus with a fast response time are required followed by the investigations of the performances with respect to the field-dependent rheological properties of a novel of bidisperse MR grease.

Declaration of conflicting interests


The author(s) declared no potential conflicts of interest with respect to the research, authorship and/or publication of this article.

Funding

The author(s) disclosed receipt of the following financial support for the research, authorship, and/or publication of this article: This research was financially supported by the

Universiti Teknologi Malaysia under the Professional Development Research University (Vot No. 04E02) and Potential Academic Staff (Vot No. 03K16) grants. The research was also partially funded by the SHERA Project Prime Award: AID-497-A-16-00004, USAID and Universitas Sebelas Maret (UNS) through Hibah Kolaborasi Internasional 2019.

ORCID iDs

Norzilawati Mohamad  <https://orcid.org/0000-0002-3113-6598>

Seung-Bok Choi  <https://orcid.org/0000-0001-6262-2815>

References

- Agirre-Olabide I and Elejabarrieta MJ (2017) Effect of synthesis variables on viscoelastic properties of elastomers filled with carbonyl iron powder. *Journal of Polymer Research* 24(9): 139.
- An H-N, Sun B, Picken SJ, et al. (2012) Long time response of soft magnetorheological gels. *The Journal of Physical Chemistry B* 116(15): 4702–4711.
- Carlson JD (2002) What makes a good MR fluid? *Journal of Intelligent Material Systems and Structures* 13(7–8): 431–435.
- Carlson JD and Jolly MR (2000) MR fluid, foam and elastomer devices. *Mechatronics* 10(4): 555–569.
- Chekanova LA, Denisova EA, Yaroslavtsev RN, et al. (2015) Micro grid frame of electroless deposited Co-P magnetic tubes. *Solid State Phenomena* 233–234: 64–67.
- De Vicente J, Klingenberg DJ and Hidalgo-Alvarez R (2011) Magnetorheological fluids: a review. *Soft Matter* 7(8): 3701.
- De Vicente J, Segovia-Guti era JP, Andablo-Reyes E, et al. (2009) Dynamic rheology of sphere- and rod-based magnetorheological fluids. *The Journal of Chemical Physics* 131(19): 194902.
- De Vicente J, Vereda F, Segovia-Guti era JP, et al. (2010) Effect of particle shape in magnetorheology. *Journal of Rheology* 54(6): 1337.
- Farmer VC (1998) Differing effects of particle size and shape in the infrared and Raman spectra of kaolinite. *Clay Minerals* 33(4): 601–604.
- G omez-Ram rez A, L pez-L pez MT, Dur n JDG, et al. (2009) Influence of particle shape on the magnetic and magnetorheological properties of nanoparticle suspensions. *Soft Matter* 5(20): 3888.
- Gordaninejad F, Miller M, Wang X, et al. (2007) Study of a magneto-rheological grease (MRG) damper. In: *Proceedings of SPIE: active and passive smart structures and integrated systems* (eds Y Matsuzaki, M Ahmadian and DJ Leo), San Diego, CA, 6 April 2007, p. 65250G. Bellingham, WA: SPIE.
- Ichwan B, Mazlan SA, Imaduddin F, et al. (2016) Development of a modular MR valve using meandering flow path structure. *Smart Materials and Structures* 25(3): 037001.
- Imaduddin F, Mazlan SA, Rahman MAA, et al. (2014) A high performance magnetorheological valve with a meandering flow path. *Smart Materials and Structures* 23(6): 065017.
- Jahan N, Pathak S, Jain K, et al. (2017) Enhancement in viscoelastic properties of flake-shaped iron based

- magnetorheological fluid using ferrofluid. *Colloids and Surfaces A: Physicochemical and Engineering Aspects* 529: 88–94.
- Jones SB and Friedman SP (2000) Particle shape effects on the effective permittivity of anisotropic or isotropic media consisting of aligned or randomly oriented ellipsoidal particles. *Water Resources Research* 36(10): 2821–2833.
- Karis TE, Kono R-N and Jhon MS (2003) Harmonic analysis in grease rheology. *Journal of Applied Polymer Science* 90(2): 334–343.
- Kavlicoglu BM, Gordaninejad F and Wang X (2013) Study of a magnetorheological grease clutch. *Smart Materials and Structures* 22(12): 125030.
- Kim JE, Ko J-D, Liu YD, et al. (2012) Effect of medium oil on magnetorheology of soft carbonyl iron particles. *IEEE Transactions on Magnetics* 48(11): 3442–3445.
- Kintz KA, Carlson D, Munoz C, et al. (2003) *Magnetorheological grease composition*. US6547986B1 Patent.
- Laherisheth Z and Upadhyay RV (2017) Influence of particle shape on the magnetic and steady shear magnetorheological properties of nanoparticle based MR fluids. *Smart Materials and Structures* 26(5): 054008.
- López-López MT, Kuzhir P, Bossis G, et al. (2008) Preparation of well-dispersed magnetorheological fluids and effect of dispersion on their magnetorheological properties. *Rheologica Acta* 47(7): 787–796.
- Luxon JT, Montgomery DJ and Summit R (1969) Effect of particle size and shape on the infrared absorption of magnesium oxide powders. *Physical Review* 188(3): 1345–1356.
- Mizes HA (1995) Surface roughness and particle adhesion. *The Journal of Adhesion* 51(1–4): 155–165.
- Mohamad N, Mazlan SA, Choi SB, et al. (2016) The field-dependent rheological properties of magnetorheological grease based on carbonyl-iron-particles. *Smart Materials and Structures* 25(9): 095043.
- Mohamad N, Ubaidillah, Mazlan SA, et al. (2018) A comparative work on the magnetic field-dependent properties of plate-like and spherical iron particle-based magnetorheological grease. *PLoS ONE* 13(4): e0191795.
- Park BJ, Fang FF and Choi HJ (2010) Magnetorheology: materials and application. *Soft Matter* 6: 5246.
- Park BO, Park BJ, Hato MJ, et al. (2011) Soft magnetic carbonyl iron microsphere dispersed in grease and its rheological characteristics under magnetic field. *Colloid and Polymer Science* 289(4): 381–386.
- Rabinow J (1948) The magnetic fluid clutch. *Transactions of the American Institute of Electrical Engineers* 67(2): 1308–1315.
- Rankin PJ, Horvath AT and Klingenberg DJ (1999) Magnetorheology in viscoplastic media. *Rheologica Acta* 38(5): 471–477.
- Rigbi Z and Jilkén L (1983) The response of an elastomer filled with soft ferrite to mechanical and magnetic influences. *Journal of Magnetism and Magnetic Materials* 37(3): 267–276.
- Sahin H, Gordaninejad F, Wang X, et al. (2007) Rheological behavior of magneto-rheological grease (MRG). In: *Proceedings of SPIE: active and passive smart structures and integrated systems* (eds Matsuzaki Y, Ahmadian M and Leo DJ), San Diego, CA, 6 April 2007, p. 65250D. Bellingham, WA: SPIE.
- Sahin H, Wang X and Gordaninejad F (2009) Temperature dependence of magneto-rheological materials. *Journal of Intelligent Material Systems and Structures* 20(18): 2215–2222.
- Sarkar C, Hirani H and Sasane A (2015) Magnetorheological smart automotive engine mount. *International Journal of Current Engineering and Technology* 5(1): 419–428.
- Segovia-Gutiérrez JP, Berli CL and de Vicente J (2012) Non-linear viscoelasticity and two-step yielding in magnetorheology: a colloidal gel approach to understand the effect of particle concentration. *Journal of Rheology* 56(6): 1429–1448.
- Shah K, Oh J-S, Choi S-B, et al. (2013) Plate-like iron particles based bidisperse magnetorheological fluid. *Journal of Applied Physics* 114(21): 213904.
- Shah K, Phu DX, Seong M-S, et al. (2014) A low sedimentation magnetorheological fluid based on plate-like iron particles, and verification using a damper test. *Smart Materials and Structures* 23(2): 027001.
- Shilan ST, Mazlan SA, Ido Y, et al. (2016) A comparison of field-dependent rheological properties between spherical and plate-like carbonyl iron particles-based magneto-rheological fluids. *Smart Materials and Structures* 25(9): 095025.
- Siebert E, Laherisheth Z and Upadhyay RV (2015) Dilution dependent magnetorheological effect of flake-shaped particle suspensions – destructive friction effects. *Smart Materials and Structures* 24(7): 075011.
- Song KH, Park BJ and Choi HJ (2009) Effect of magnetic nanoparticle additive on characteristics of magnetorheological fluid. *IEEE Transactions on Magnetics* 45(10): 4045–4048.
- Sukhwani VK and Hirani H (2008) A comparative study of magnetorheological-fluid-brake and magnetorheological-grease-brake. *Tribology Online* 3(1): 31–35.
- Ubaidillah, Mazlan SA, Sutrisno J, et al. (2014) Potential applications of magnetorheological elastomers. *Applied Mechanics and Materials* 663: 695–699.
- Upadhyay RV, Laherisheth Z and Shah K (2014) Rheological properties of soft magnetic flake shaped iron particle based magnetorheological fluid in dynamic mode. *Smart Materials and Structures* 23(1): 15002.
- Wang W, Guo J, Long C, et al. (2015) Flaky carbonyl iron particles with both small grain size and low internal strain for broadband microwave absorption. *Journal of Alloys and Compounds* 637: 106–111.
- Wenyan L, Yingying Z and Xin Y (2015) *Effects of Ball Milling Process on the Electromagnetic Parameters of Carbonyl Iron Powder* (Material Application in EMC). Available at: <http://www.semc.cesi.cn/backend/pics/files/File/2015/semc2015en07.pdf>
- Wilson R, Dini D and Van Wachem B (2017) The influence of surface roughness and adhesion on particle rolling. *Powder Technology* 312: 321–333.
- Xu Y, Gong X and Xuan S (2013) Soft magnetorheological polymer gels with controllable rheological properties. *Smart Materials and Structures* 22(7): 075029.
- Yang P, Yu M, Fu J, et al. (2017) Rheological properties of dimorphic magnetorheological gels mixed dendritic carbonyl iron powder. *Journal of Intelligent Material Systems and Structures* 29: 12–23.